Theoretical and Applied Climatology (2024) 155:2997–3012
https://doi.org/10.1007/s00704-023-04772-y

RESEARCH

Analysis of drought intensity, frequency and trends using the spei in Turkey

Hıdır Serkendiz[1] · Hasan Tatli[1] · Ayşegül Kılıç[1] · Mahmut Çetin[2] · Ali Sungur[3]

Received: 8 May 2022 / Accepted: 27 November 2023 / Published online: 20 December 2023
© The Author(s), under exclusive licence to Springer-Verlag GmbH Austria, part of Springer Nature 2023

Abstract

This study addresses into the critical issue of drought as a natural disaster, especially in regions characterized by arid and semi-arid climates like Turkey. The primary aim of this study is to investigate the historical occurrences of meteorological drought events in Turkey, focusing on their past frequency, intensity, and spatial distribution. The study employs the Standardized Precipitation Evapotranspiration Index (SPEI) method and utilizes 50 years of monthly temperature and precipitation data collected from 222 meteorological stations across the country. Drought severity is assessed using the run theory method, and trends in drought patterns are analyzed through the Mann–Kendall trend test. Additionally, the text explores the connection between elevation and the geographical distribution of drought events.

The study's findings reveal a noticeable increase in the occurrence of drought periods over time. Among the selected periods, the most widespread drought event was observed in the year 2001. The Bozcaada meteorology station exhibited the highest frequency of drought with a value of 223, while the Ispir meteorology station recorded the lowest frequency with a value of 151. Over the course of the 50-year analysis, no significant correlation was found between drought and elevation, although a gradual increase was noted in the last 10 years. The results also indicate a gradual north-to-south increase in drought intensity in Turkey. The study identifies four distinct drought hotspots in the country: the Western Anatolia Region, Central and Southern Anatolia Region, Southeastern Anatolia Region, and Eastern Anatolia Region.

Keywords Mann–Kendall · Mediterranean · Meteorological Drought · SPEI · Run Theory, Turkey

1 Introduction

Drought, an escalating global concern, represents a natural hazard with far-reaching implications, affecting ecosystems, agriculture, water resources, and human livelihoods. As highlighted by Mishra and Singh (2010), drought has historically exerted profound social and economic impacts on millions of people worldwide. Recent data from the Center for Research on the Epidemiology of Disasters (CRED), drawing from EM-DAT records, reveal that between 2000 and 2019, approximately 1.5 billion people on the African continent alone experienced adverse effects due to drought (CRED 2020). Projections from the Intergovernmental Panel on Climate Change (IPCC) in 2021 indicate that the world can expect significant increases in drought intensity, duration, and geographic extent (IPCC 2021). Furthermore, the UNDRR 2022 report suggests that if current trends persist, drought events are estimated to increase by roughly 30% on a global scale by 2030 (UNDRR 2022).

While there is no universally agreed-upon definition of drought, Wilhite (2000) generally characterizes it as a natural reduction in precipitation over an extended period, such as a season or longer. Drought is unique as a "slow-moving" natural disaster that can occur in nearly all climate types, with unpredictable start and end dates (Tatli and Dalfes 2020). Wilhite (1993) distinguishes drought from other natural hazards in several ways: its gradual onset and resolution make pinpointing the exact timing challenging, there is no universally applicable definition, and the impacts, typically non-structural, spread over large geographic areas.

✉ Hıdır Serkendiz
hserkendiz@gmail.com

[1] Department of Geography, Canakkale Onsekiz Mart University, 17020 Canakkale, Turkey

[2] Department of Agricultural Structures and Irrigation, Faculty of Agriculture, University of Cukurova, Adana, Turkey

[3] Soil Science and Plant Nutrition Department, Canakkale Onsekiz Mart University, 17020 Canakkale, Turkey

While the impact of drought heavily depends on the vulnerability of the affected community (Wilhelmi and Wilhite 2002), a thorough drought analysis necessitates examining its physical or exposure aspects. Various methods with different approaches and prerequisites have been developed to analyze the physical attributes of drought -intensity, duration, and spatial extent- (Baydaroğlu Yeşilköy et al. 2021). Widely used indices for examining drought characteristics include the Palmer Drought Severity Index (PDSI), devised by Palmer (1965), which combines monthly or weekly average temperature, total precipitation, soil moisture, and potential evapotranspiration data. The Standardized Precipitation Index (SPI), developed by McKee and Doesken (1993), standardizes precipitation amounts for a specific period, transforming them into a normal distribution with a fixed mean and standard deviation. Another essential index is The Standardized Precipitation Evapotranspiration Index (SPEI), created by Vicente-Serrano et al. (2010), which incorporates evaporation data into the precipitation-based calculations. SPEI, by considering temperature, can better capture the impact of surface evaporation changes, which are sensitive to drought responses induced by global warming (Liu et al. 2021). Apart from these widely used indices, numerous others have been developed for drought analysis (Tatli and Türkeş 2011; Zarei and Mahmoudi 2021; Zarei et al. 2023a, b).

Turkey's climate is primarily shaped by prevailing atmospheric masses, influenced by its geographical position. The country's specific location and physiographic conditions significantly diversify its climate. Most of Turkey falls under the Mediterranean Macro Climate influence, prevalent on the western coasts of continents at similar latitudes. This climate encompasses arid, semi-arid, and semi-humid conditions observed throughout much of Turkey, marked by an annual water deficit and soil moisture deficiency. Various climate classification studies conducted in Turkey support this classification (Peel et al. 2007; Tekin et al. 2021). Furthermore, studies based on climate change scenarios indicate an anticipated increase in the intensity, frequency, and duration of drought events in Turkey's future climate conditions (Sen et al. 2012; Turp et al. 2014). In summary, Turkey is exposed to significant and severe drought risks under current and projected climate conditions.

Numerous studies have employed diverse methodologies to investigate the temporal and spatial characteristics of historical drought conditions in Turkey. For instance, Türkeş and Tatli (2009) proposed and implemented a novel approach based on the SPI methodology recommended by McKee and Doesken (1993) to assess the temporal and spatial dimensions of drought events in Turkey. Türkeş et al. (2009) used the PDSI approach to analyze drought characteristics in Konya, a city in central Turkey. Tatli (2015a) utilized statistical downscaling and the SPI approach to explore the potential impacts of climate change on meteorological drought periods in Turkey. Tatli and Türkeş (2011) applied PDSI and the Palmer Hydrological Drought Index at the national level in Turkey, incorporating Empirical Orthogonal Functions models. Tatli and Dalfes (2020) utilized the trend-free fluctuation analysis method for SPI, investigating the spatiotemporal properties of drought persistence across Turkey.

This paper aims to provide a comprehensive examination of the frequency, intensity, and spatial extent of meteorological drought in Turkey based on an extensive dataset spanning from 1970 to 2019, collected from 222 national-scale meteorological stations. The study employs the SPEI method for this research, chosen for its inclusion of not only precipitation but also temperature and potential evapotranspiration (PET) in drought calculations. As a result, SPEI, by considering temperature, can capture the effects of changes in surface evaporation, which are more sensitive to drought responses induced by global warming (Liu et al. 2021). Another objective of this research is to investigate the temporal and spatial correlation between drought and elevation in Turkey. Turkey's rugged topography features substantial elevation variations over short distances compared to its immediate surroundings. In this context, the novelty of this study lies in the comprehensive analysis of drought characteristics using the SPEI approach at a national scale. Additionally, this research represents the first attempt to analyze the relationship between drought and elevation in Turkey.

In line with the objectives of this study, the paper's general structure is organized as follows: First, SPEI values at a 12-month scale are computed based on monthly temperature and precipitation data. Subsequently, drought duration and intensity are calculated in 10-year periods, employing the run theory approach for this calculation. Spatial pattern models of drought are then established. Finally, the Mann–Kendall (M–K) trend test is used to evaluate drought trends statistically, identifying potentially significant drought trends.

2 Methodology and data

2.1 Data and research area

The data used in this study was generously provided by the Turkish State Meteorological Service. It consists of monthly temperature (°C) and monthly total precipitation (mm/month) time series. The dataset spans over 50 years, encompassing data from 222 meteorological stations located across Turkey, ranging from 1970 to 2019.

While there is not a specific guideline in the existing literature determining the data gap rate in time series, it is being conventionally practiced to empirically use a range of 5% to

10% (Schneider 2001; Junninen et al. 2004; Moral 2010; Hamzah et al. 2021). For this research, we opted for station data with a maximum of 7% missing data at each weather station and employed the kriging method (Matheron 1963; Cressie 1990) to fill in the gaps. Additionally, when addressing the missing monthly temperature data, we factored in the elevations of neighboring stations and considered the temperature variation with altitude, assuming a rate of -6.5 °C per kilometer. Kriging was originally developed for mining purposes based on core samples (Matheron 1963; Cressie 1990).

In addition to addressing data gaps, the monthly temperature and annual precipitation data underwent rigorous testing. The following homogeneity tests were applied: Pettitt, Standard normal homogeneity, Buishand, and von Neumann. Stations that passed at least two of these four tests with a p-value exceeding 0.05 were considered homogeneous. Consequently, the data from 31 stations for yearly precipitation and 18 stations for monthly temperature were identified as non-homogeneous. It is noteworthy that the von Neumann test yielded non-homogeneous results for temperature data across all stations.

For spatial representation, the inverse distance weighted (IDW) approach was adopted to interpolate long-term total average precipitation data and SPEI values onto a grid. The spatial distribution of these stations is depicted in Fig. 1.

Data analysis, SPEI computation, and visualization were performed using the R- programming language, with maps generated through ArcGIS Pro version 2.8.

Turkey's geographical layout extends from 36 to 42 degrees north latitudes and from 26 to 45 degrees east longitudes, forming a pseudo-rectangular shape in the east–west direction. The country is geographically divided into two major peninsulas: Thrace and Anatolia. Thrace, located in western Turkey, presents a relatively uniform topography with an average elevation of approximately 160 m. In contrast, the Anatolian peninsula, covering 97% of the nation's land area, features a rugged terrain with an average elevation of around 1170 m. The eastern sections of Anatolia exhibit elevations surpassing 2000 m, while the north–south mountain ranges in the north and south exceed 3000 m (Koç 2013).

Turkey's climate is predominantly influenced by the "Mediterranean Macro-climate," which prevails along the western coasts of continents at similar latitudes (Erinç 1993). However, there are distinct sub-climate types with unique characteristics, primarily determined by geographic proximity to seas and physical topographic variables such as orography, elevation, aspect, and continentality.

2.2 Standardized precipitation evapotranspiration index

According to the methodology established by Vicente-Serrano et al. (2010), the Standardized Precipitation Evapotranspiration Index (SPEI) is computed through the utilization of a water-deficit parameter denoted as D. This parameter (D) is derived



Fig. 1 Study area location and geographical distribution of weather stations: MAR stands for Marmara Region, AR stands for Aegean Region, MEDR stands for Mediterranean Region, CAR stands for Central Anatolia Region, BSR stands for Black Sea Region, EAR stands for Eastern Anatolia Region, and SEAR stands for Southeast Anatolia Region

by subtracting the potential evapotranspiration (PET) from the observed precipitation (P) on a monthly basis. Mathematically, this relationship is expressed as follows:

$$D_i = P_i - PET_i \tag{1}$$

where D_i representswater deficit, P is the precipitation, and PET is the potential evapotranspiration for i-th month. This calculation is performed for each month to determine the monthly values of the standardized precipitation evapotranspiration index. The SPEI calculation commences with the computation of PET, which is determined through the empirical approach formulated by Thornthwaite (1948). PET is calculated as:

$$PET = dl\ 16\left(\frac{10T}{I}\right)^b \tag{2}$$

here, *dl* is a latitude-dependent correction factor to calculate day length, *T* is the monthly mean temperature (°C), and *I* is the heat index, which aggregates the 12-month heat index calculated as:

$$I = \sum_{j=}^{12}\left(\frac{T}{T}\right)^{1.514} \tag{3}$$

The constant "b" in Eq. 2 is determined by the following equation:

$$b = 6.75\times10^{-7}\cdot \mathrm{I}^3 - 7.71\times10^{5}\cdot \mathrm{I}^2 + 1.79\times10^{-2}\cdot \mathrm{I} + 0.49 \tag{4}$$

The subsequent step involves fitting the D_i values to a probability density function, much like the SPI, followed by the computation of drought indices in the second stage using the inverse standardized normal distribution. While the SPI typically utilizes the Gamma distribution for precipitation values, Vicente-Serrano et al. (2010) suggest the use of a log-logistic distribution, described as:

$$f(x) = \frac{\beta}{a}\left(\frac{x-\gamma}{a}\right)^{\beta-1}\left[1+\left(\frac{x-\gamma}{a}\right)^{-2}\right] \tag{5}$$

The parameters α, β, and γ for the log-logistic distribution can be derived using the L-moment approach, outlined in Eqs. 6, 7, and 8.

$$\beta = \frac{2w_{1_}w_0}{6w_1 - w_0 - 6w_2} \tag{6}$$

$$a = \frac{\left(w_0 - 2w_1\right)\beta}{\Gamma(1+1/\beta)\Gamma(1-1/\beta)} \tag{7}$$

$$\gamma = w_0 - a\Gamma\left(\frac{1+1}{\beta}\right)\Gamma\left(\frac{1-1}{\beta}\right) \tag{8}$$

Here, Γ represents the Gamma function, and w_s is the probability density function computed as:

$$w_s = \frac{1}{N}\sum_{i=1}^{N}\left(1-F_i\right)^5 D_i \tag{9}$$

where F_i is an empirical frequency, and F_i is defined as:

$$F_i = \frac{i-0.35}{N} \tag{10}$$

The "i" signifies the increasing number of observation intervals, and "*N*" is the length of the data. The probability distribution function of the D series is established through the log-logistic distribution as shown in Eq. 11.

$$F(x) = \left[1+\left(\frac{a}{x-\gamma}\right)^{\beta}\right]^{-1} \tag{11}$$

The SPEI value is computed according to:

$$SPEI = W - \frac{C_0 + C_1 W + C_2 W^2}{1 + d_1 W + d_2 W^2 + d_3 W^3} \tag{12}$$

where W is defined as:

$$W\sqrt{\ } = \begin{matrix}\sqrt{-2In(P)}\ for\ P \le 0.5 \\ \sqrt{-2\ln(1-\mathrm{P})}\ for\ P > 0.5\end{matrix}\Bigg\} \tag{13}$$

The parameter *P* represents the probability of exceeding a given *D* value. The constants C_0, C_1, C_2, d_1, d_2, and d_3 are the coefficients in Eq. 12. The classification of SPEI values into drought categories is detailed in Table 1.

Furthermore, the selection of a 12-month time scale for assessing meteorological drought in Turkey is primarily based on the region's significant seasonal variations, influenced by the prevailing Mediterranean climate. This climate pattern manifests as low precipitation and high temperatures in the summer months, contrasting with higher precipitation during the winter months. The 12-month time scale is ideal for capturing these annual fluctuations in precipitation and evaporation data. Additionally, the one-year period aligns with the planning cycles of the agricultural sector and water resources management. Agriculture and

Table 1 The Standard Precipitation Index and the Standard Precipitation and Evapotranspiration Index values and classes (Liu et al. 2021)

SPEI Values	Drought Class
≥2	Extremely wet
1.5–1.99	Vert wet
1–1.49	Moderately wet
-0.99–0.99	Near-normal
-1–1.49	Moderately dry
-1.5–1.99	Vert dry
≤-2.00	Extremely dry

water reservoir management are typically organized on an annual basis, making the 12-month SPEI a valuable tool for assessing long-term drought trends crucial for agriculture and water resource management. Furthermore, the 12-month time scale facilitates the evaluation of long-term processes like climate change in Turkey, which is essential for monitoring trends, predicting future drought risks, and implementing appropriate measures.

2.3 The theory of runs

Droughts are characterized by their duration, intensity, and frequency. In this study, the run theory method developed by Yevjevich (1967) was employed to calculate drought intensity. This method defines drought intensity as a segment of a time series where all values are consistently above or below a selected threshold, whether negative or positive. In this study, drought intensity is computed as follows:

$$I = \frac{\sum_{n=1}^{T} |I_{SPEI} - K|}{T} \tag{14}$$

here, K represents the threshold value, which is set at -0.5 in this case. I_{SPEI} is the count of SPEI values below this threshold, T is the duration of the drought, and I signifies the intensity of the drought. Additionally, drought frequency, reflecting the recurrence of drought, is calculated as follows:

$$F = \frac{m}{N} \tag{15}$$

where N represents the observation period, m represents the count of droughts (SPEI < -0.5) during that period, and F denotes the frequency of drought occurrences.

2.4 Mann–Kendall trend test

To derive statistical insights from the patterns, we also employed the M–K trend analysis, as described by Hirsch et al. (1991). The M–K trend test is a non-parametric statistical test originally introduced by Mann (1945), subsequently enhanced by Kendall (1975), and further refined by Hirsch et al. (1991). The initial step in applying the M–K trend test involves establishing the following hypotheses (Tatli 2015b):

Formulation of the null (H_0) and alternative (H_a) hypotheses:

H_0: There is no trend in the series
H_a: There is a trend in the series

Calculate the test statistic, F, required for null hypothesis testing, as defined in Eq. 16:

$$F = \sum_{i=1}^{N-1} \sum_{j=i+1}^{N} sgn(X_j - X_i) \tag{16}$$

In this equation, sgn is the signal function, which is defined as follows:

$$sgn = \begin{cases} 1, & a > b \\ 0, & a = b \\ -1, & a < b \end{cases} \tag{17}$$

The following equation is used to calculate the variance of a test statistic with zero average and normal distribution.

$$Var(F) = \frac{N(N-1)(2N+5) - \sum_{i=1}^{k} t_i(i)(i-1)(2i+5)}{18} \tag{18}$$

where ti denotes the number of samples in the *i-th* sample. Finally, the Z-test statistic is computed using the expression below:

$$Z = \begin{cases} \frac{F-1}{Var(F)}, & F > 0 \\ 0, & F = 0 \\ \frac{F+1}{Var(F)} & F < 0 \end{cases} \tag{19}$$

Here, it is assumed that the Z statistic follows a normal distribution. A trend is considered statistically significant at a given confidence level, typically 1-α/2, if the Z value is greater than the Z_1-α/2 value, where α indicates the level of significance, commonly taken as 0.05 (5%) or 0.01 (1%). The direction of the trend, whether positive or negative, is determined by the signal of the F statistic.

It is important to emphasize that the M–K test is employed to identify trends present in the time series data.

3 Results

The precipitation distribution map of Turkey, illustrated in Fig. 2, provides insight into the country's average annual rainfall patterns. Notably, regions along the coastline, especially those bordering the Black Sea, experience the highest levels of precipitation. Among these, the Eastern Black Sea Section stands out, receiving over 2000 mm of rainfall annually. Additionally, provinces like Giresun, Ordu, Bartin, and Zonguldak, situated in the central and western parts of the Black Sea Region, receive substantial rainfall, surpassing 900 mm. Beyond the Black Sea Region, the provinces of Mugla, Antalya, and Hatay in the Mediterranean Region record significant precipitation exceeding 900 mm. In contrast, provinces such as

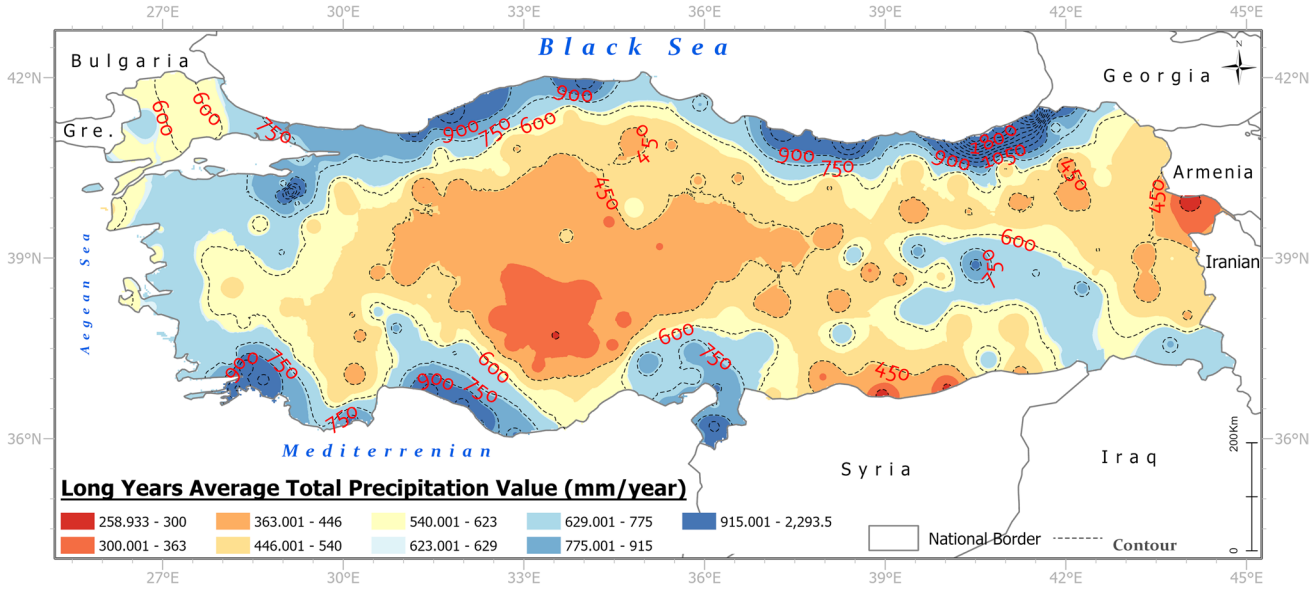


Fig. 2 Long-term mean of total precipitation values in Turkey from 1970 to 2019

Igdir in the east, Sanliurfa in the southeast, and Konya in Central Anatolia exhibit markedly lower precipitation levels, measuring 320 mm or less. Igdir, in particular, witnesses the lowest precipitation in Turkey, averaging merely 260 mm annually. This diverse distribution emphasizes the considerable variation in rainfall across Turkey, with coastal areas and specific regions receiving ample precipitation while inland and eastern areas experience significantly drier conditions.

3.1 SPEIs for a selection of stations and years

Figure 3 illustrates the SPEI values for 222 meteorology stations across Turkey. This graph showcases the temporal variations in SPEI values at eight stations (their locations are indicated in Fig. 1) spanning Turkey's seven major geographic regions. Generally, from 1970 to 2019, dry and wet seasons alternate, with the driest decade observed across all selected stations being nearly between 2000 and

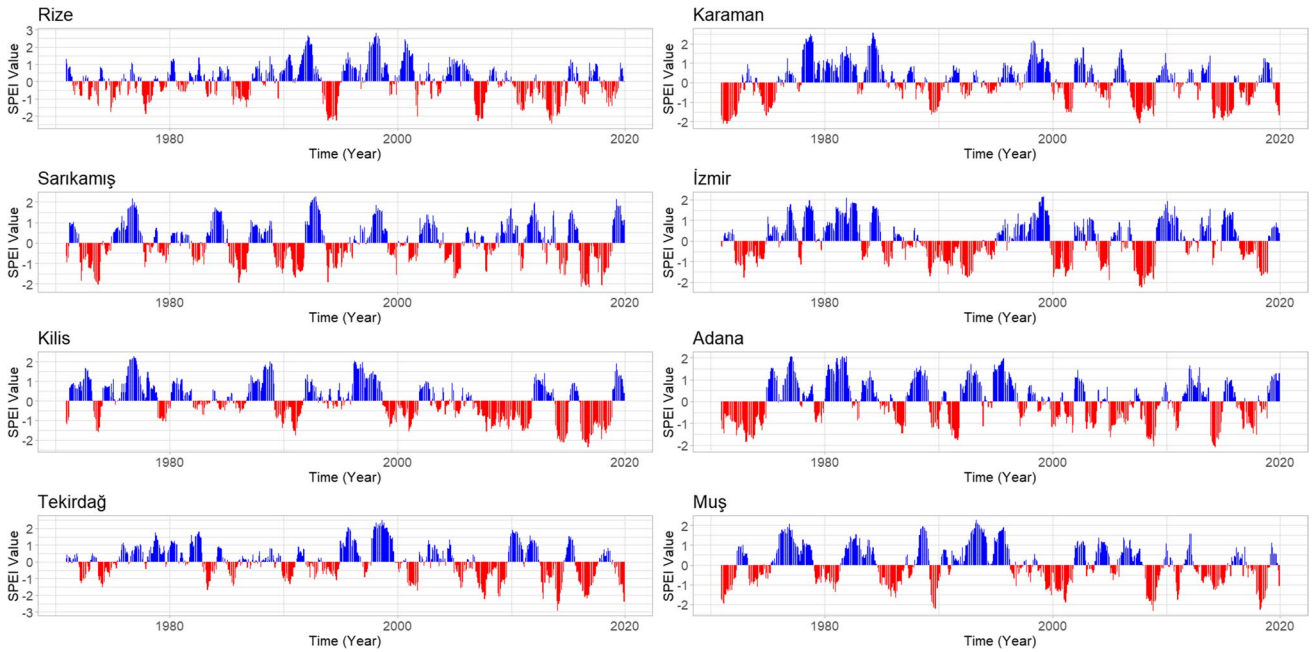


Fig. 3 Time patterns of SPEI-12 values at selected stations. The information about the stations' locations is depicted in Fig. 1

2010. Notably, the most severe drought occurred in 2013 at the Tekirdag station, while the most humid periods were recorded at the Rize station in 1991 and 1992, as well as in 1998 and 1999. In order to enhance the interpretation of the dry periods depicted in Fig. 3, emphasis is placed on the very dry (-1.5 to -1.99) and extremely dry (< -2) classes throughout the time series. In this context, the most drought years observed during the analyzed dates are summarized in Table 2 for the eight selected stations. According to the information summarized in the table, significant severe droughts were experienced across all stations during the time series. Furthermore, it can be stated based on these findings that each station faced an average of 11 years of severe drought over the examined 50-year period. Among these stations, the station with the shortest duration of severe drought was Adana, with 9 years, whereas Sarikamis station recorded the longest duration, with 13 years.

Taking these dry years into account, the 1970–1975, 1985–1995, and 2000–2019 periods were all dry years for almost all stations. The key point here is that the length of the dry periods gradually increased as the series progressed to the present. In other words, the first period lasted five years (1970–1975), the second period ten years (1985–1995), and the third period twenty years (200–2019). Rising evapotranspiration rates associated with rising global temperatures can explain the gradual extension of drought periods.

Figure 4 and 5 illustrate the spatial distribution patterns of the six driest years (1973, 1989, 1993, 1994, 2001, and 2008) occurring throughout the time series, based on the literature. (Akbaş 2014; Türkeş 1990). To represent drought patterns in a seasonal context, the months of February for winters and July for summers are used. In this context, Fig. 4 depicts the SPEI values for February and July in 1973, 1989, and 1993.

Drought conditions were "near-normal" in the majority of regions across Turkey in February (Fig. 4a) and July (Fig. 4b) of 1973. When comparing February and July of 1973, it can be concluded that July is the driest month. While most of Turkey is "near-normal" in July, the majority of the Southeastern Anatolia Region, the western part of the Eastern Anatolia Region, the central and eastern parts of the Mediterranean Region, and the southwestern part of Konya are "moderately dry", with some areas being "extremely dry". The province of Hakkari, located in Turkey's southeast corner, is particularly "very dry" and "extremely dry" in 1973.

Looking at February (Fig. 4c) and July (Fig. 4d) in 1989, it can be concluded that July is the driest.

The conditions observed throughout Turkey in February 1989 are depicted in Fig. 4c. During this period, the southwest, west, and northwest regions exhibited "near-normal" drought conditions, while at the same time, the central, northern, and eastern regions displayed "moderately wet" and "very wet" conditions. It should be noted that during this period, certain areas around Bursa and Izmir experienced "moderately dry" and "very dry" conditions intermittently.

The spatial distribution of drought conditions experienced in July 1989 is illustrated in Fig. 4d. This distribution pattern reveals that the western and central-western regions were predominantly characterized by "moderately dry" and "very dry" conditions. A similar pattern was observed in the southern and southeastern regions of the country. On the other hand, the rest of the country, particularly in Central Anatolia, generally experienced drought conditions at a "near-normal" level. During this period, the northwestern region, specifically Rize, experienced "very wet" and "extremely wet" conditions.

Figure 4e and 4f depict the drought distribution for February and July in the year 1993, respectively. In both months, it is generally observed that the country experienced prevailing conditions of "near-normal", "moderately wet", and "very wet". However, it should be noted that during these time frames, certain areas in the northwestern regions exhibited occasional characteristics of "moderately dry".

Figure 5 shows SPEI values for February and July of 1994, 2001, and 2008. Figure 5a and 5b illustrate the spatial distribution of drought conditions in February and July in the year 1994, respectively. In February, the northwestern region exhibited characteristics of "moderately dry" and "very dry", whereas the southeastern region indicated "moderately wet" and "very wet" conditions. Other regions

Table 2 Significant drought years between 1970 and 2019 at selected stations. Very dry (-1.5—-1.99) and extremely dry (< -2) SPEI classes were selected as filters in the selection of these years

Stations	Significant Drought Years
Rize	1974, 1977, 1986, 1993, 1994, 2001, 2006, 2007, 2010, 2011, 2013 and 2014
Sarıkamis	1972, 1973, 1986, 1989, 1990, 1991, 1993, 1999, 2005, 2014, 2016, 2017 and 2018
Kilis	1973, 1990, 1991, 2001, 2007, 2011, 2014, 2016, 2017, and 2018
Tekirdag	1974, 1983, 2001, 2005, 2007, 2008, 2009, 2012, 2013, 2014, 2016 and 2019
Karaman	1970, 1971, 1972, 1974, 1975, 1989, 2001, 2007, 2008, 2014, 2015 and 2019
Izmir	1972, 1989, 1990, 1992, 2000, 2001, 2005, 2007, 2008 and 2018
Adana	1972, 1973, 1991, 2005, 2008, 2009, 2013, 2014 and 2017
Mus	1971, 1985, 1986, 1989, 1999, 2001, 2008, 2009, 2011, 2017 and 2018

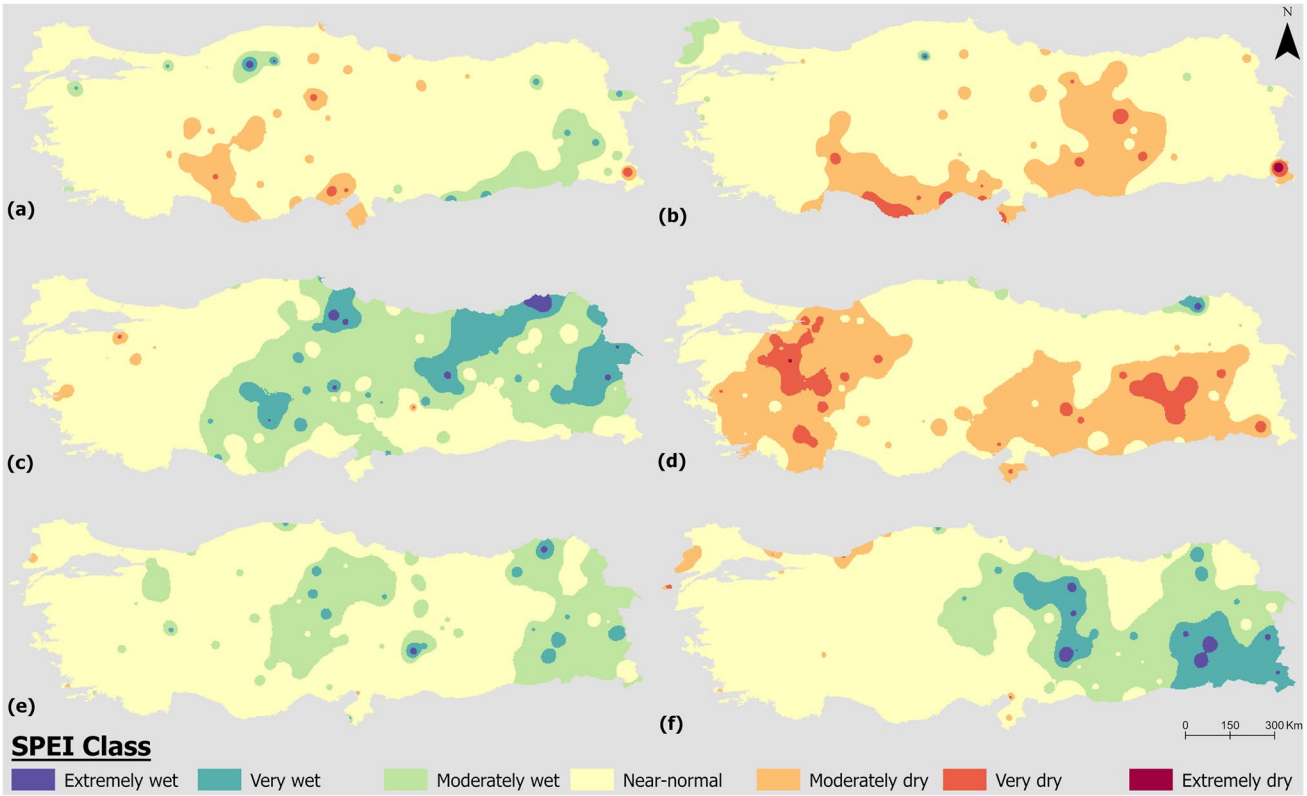


Fig. 4 SPEI-12 values from 1973, 1989, and 1993. (**a**) February 1973, (**b**) July 1973, (**c**) February 1989, (**d**) July 1989, (**e**) February 1993, and (**f**) July 1993 are shown respectively

generally experienced drought conditions at a "near-normal" level.

Figure 5c and 5d represent the drought conditions in February and July in the year 2001, respectively. Through the comparison made between the selected years, it can be stated that the most extensive spatial coverage of severe drought occurred in 2001, particularly in July. In February, spatially widespread "moderately dry", "very dry", and "extremely dry" conditions were observed in the eastern and partially western regions of the country. The central, southern, and northwestern regions generally experienced drought conditions at a "near-normal" level. The spatial distribution depicted in Fig. 5d for July 2001 represents the most severe period of drought among the selected years. Except for some areas in the eastern regions and the southeastern, nearly all other regions of the country experienced "moderately dry", "very dry", and "extremely dry" conditions. These severe drought conditions were concentrated spatially in the central, western, and northwestern regions.

Finally, Fig. 5e and 5f, respectively depict the spatial distributions of drought conditions in February and July in the year 2008. In February, the western and partially central regions of the country generally exhibited "moderately dry" and "very dry" characteristics. Conversely, narrow segments in the northwestern region observed "moderately wet" and "very wet" classifications. Other regions generally have characteristics of "near-normal" drought conditions. In July, the most severe drought is concentrated spatially in the southeastern region. Almost the entire region exhibits characteristics of "very dry" and "extremely dry". Additionally, in a significant portion of the central and western regions, "moderately dry" and "very dry" classifications are observed. Other regions generally have characteristics of "near-normal" conditions.

3.2 Spatial and temporal variation of drought frequency

Drought frequencies were calculated over ten-year periods from 1970 to 2019. In this case, those with SPEI values below -0.5 were considered drought. The station with the highest frequency, 223, is Bozcaada, located in northwest Turkey. The Ispir station, located in the northeast of Erzurum province, has the lowest frequency value of 151. The average frequency value is approximately 190, as shown in the histogram in the lower right corner of Fig. 6, and the median value is 191. Figure 6 depicts the spatial

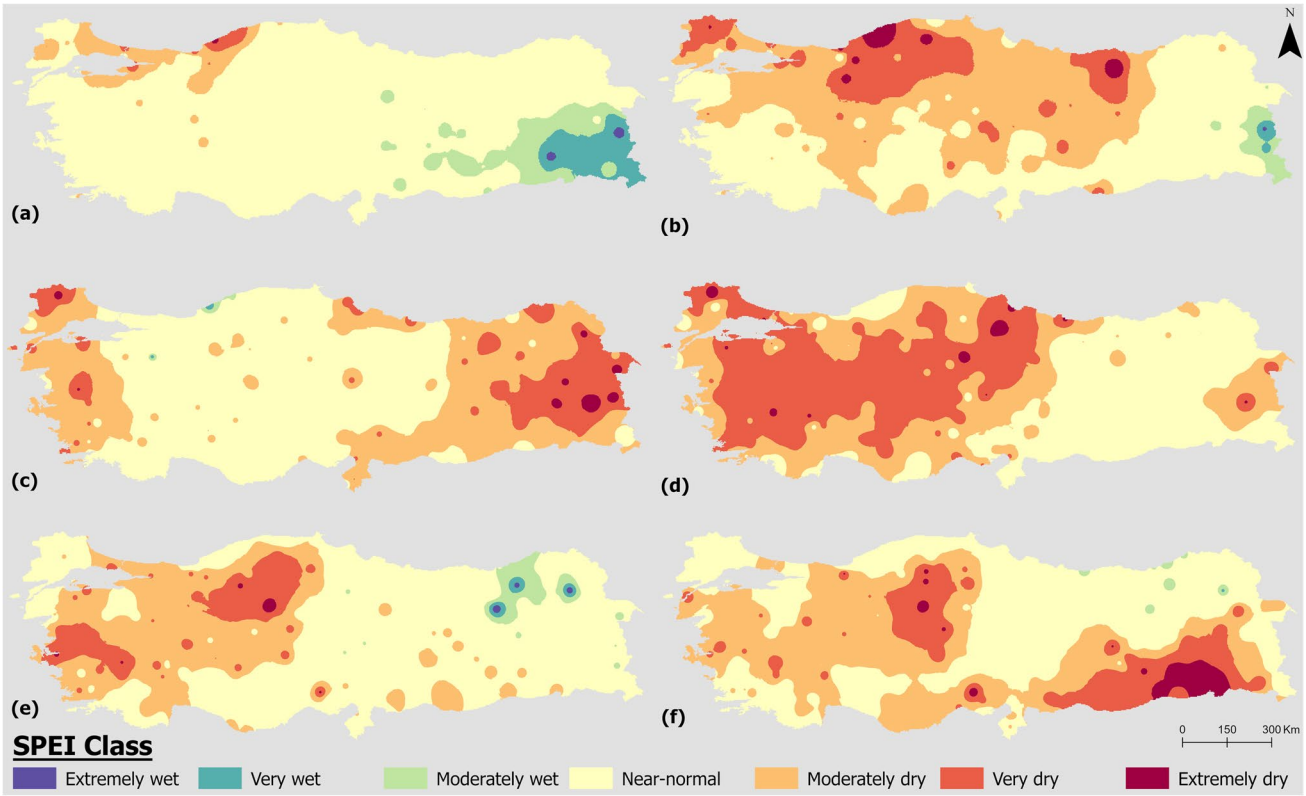


Fig. 5 Values of the SPEI-12 in 1994, 2001, and 2008. (**a**) February 1994, (**b**) July 1994, (**c**) February 2001, (**d**) July 2001, (**e**) February 2008, and (**f**) July 2008 are depicted respectively

distribution of drought frequency over ten-year periods. Overall, the findings indicate an inconsistent spatial distribution of frequencies analyzed based on ten-year time intervals. In other words, the spatial distribution pattern of frequencies changes in each period.

When examining the spatial distribution of drought frequency between 1970 and 1979, as depicted in Fig. 6a, it is observed that during this period, the highest frequency values are generally concentrated in the Central and Eastern Black Sea Region. Additionally, high-frequency values have been observed in the provinces of Konya, Isparta, Adana, Hatay, Tunceli, Diyarbakir, Hakkari, and Kars. On the other hand, regions including the northwestern part, as well as the Central, Southern, and Southeastern Anatolian Regions, exhibit relatively low-frequency values. From 1980 to 1989 (Fig. 6b), the highest frequency values are clearly observed in the western regions. Particularly, the northwestern Anatolian Region stands out as a significant area where densely clustered stations with high frequencies are observed. Similarly, the northeastern Anatolian Region is another area where high values are concentrated. On the other hand, during this period, the central and southeastern regions exhibited low-frequency values.

During the period from 1990 to 2000 (Fig. 6c), it is observed that the highest frequency values are significantly concentrated in the southwestern and western regions of the country. Except for a few stations located in the northwestern region, generally low values are observed in the rest of the country during this period. Particularly, the Central Anatolian Region stands out as the area where the lowest frequency values are observed.

From 2000 to 2009 (Fig. 6d), the region where high-frequency values are significantly concentrated includes the Central Anatolian and Eastern Mediterranean Regions. Apart from these areas, while the northwestern region occasionally shows high values, the remaining regions are generally associated with low-frequency values. Particularly, the eastern and northeastern regions stand out as the areas where the lowest frequency values are observed.

Finally, from 2010 to 2019 (Fig. 6e), the Anatolian high plateau, encompassing a vast geographical area including the eastern part of Central Anatolia and Eastern Anatolia, emerged as a region where high-frequency values are significantly concentrated. Areas outside of this extensive region are generally characterized by low-frequency

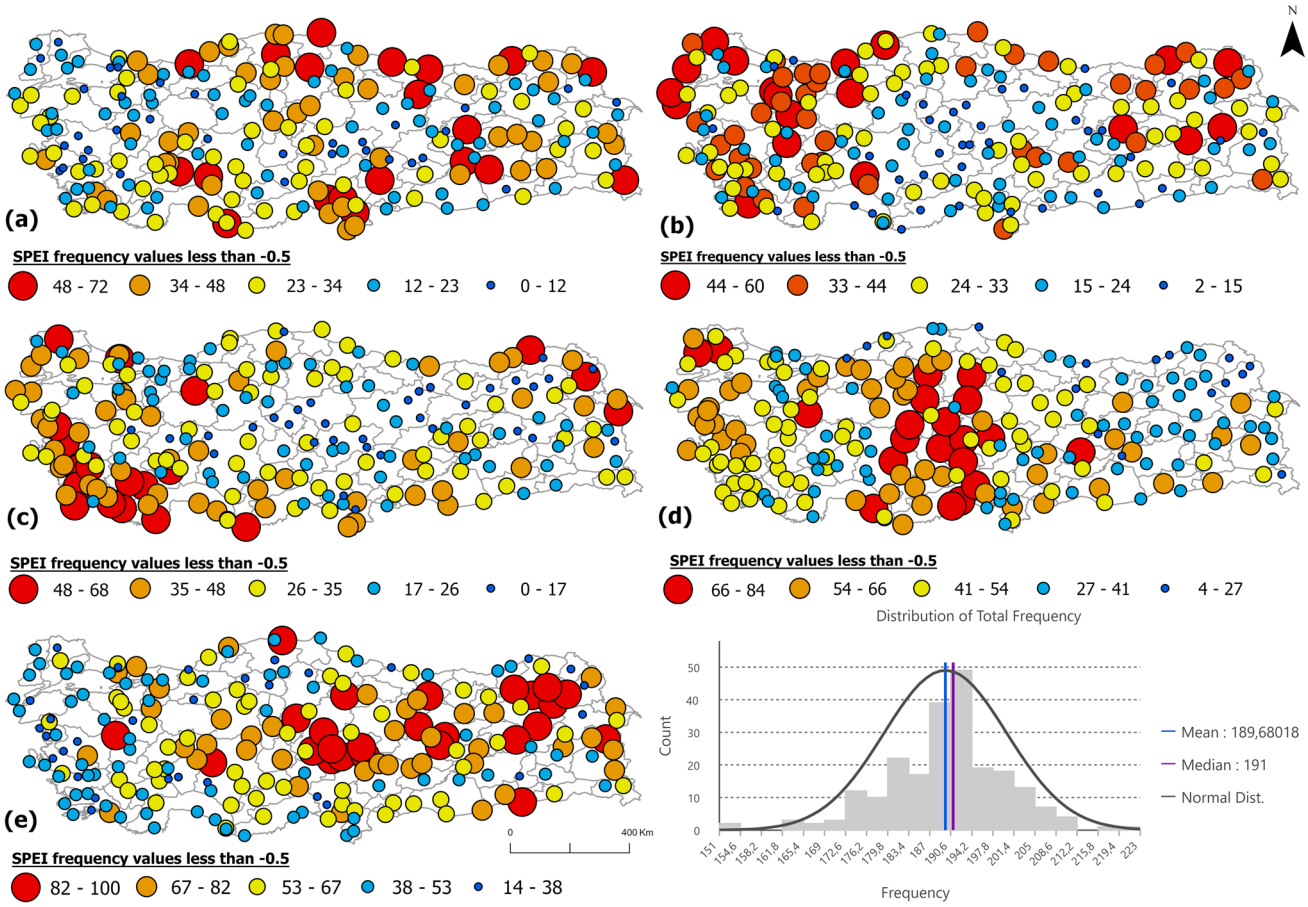


Fig. 6 SPEI-12 values less than -0.5. (**a**) 1970–1979, (**b**) 1980–1989, (**c**) 1990–2000, (**d**) 2000–2009, and (**e**) 2010–2019, and the histogram illustrates the distribution of total frequencies from 1970 to 2019

values. Especially, the western part of Anatolia stands out as the region where the lowest frequency values are observed during this period. Figure 7 illustrates how SPEI values change over time with elevation. According to the findings, a significant portion of drought events occurs at elevation levels ranging from 0–200 to 500–1250 m throughout all periods. Particularly, the elevation range of 0–200 m, which includes coastal areas, is the most distinct cluster level. Another clustering range includes elevations of 500–1250 m, common in low and moderate-altitude plateaus. In this context, it is difficult to assert a significant relationship between drought and elevation during the ten-year periods between 1970 and 2009. However, from 2010 to 2019, a gradually increasing drought trend is observed as elevation increases. This finding is clearly depicted in Fig. 6e, illustrating the spatial distribution of drought frequencies during the 2010–2019 period. Drought events are most frequently observed in the eastern region of Anatolia, characterized by high mountains and plateaus.

3.3 Spatial pattern of drought intensity

Drought intensity was calculated using the run theory approach based on SPEI values. The spatial distribution of the findings is presented in Fig. 8. According to the results, drought intensity gradually increases from north to south across Turkey. In this context, the western, central, southern, and eastern regions of the country generally exhibit high drought intensity. On the other hand, the Black Sea Region, the Marmara Region, and the northwestern part of Central Anatolia indicate low drought intensity.

Additionally, from a spatial distribution perspective, the drought intensity prominently highlights four regions identified as hotspots using a subjective approach. The first region is the *Western Anatolia Region*, encompassing the entire Aegean Region and partially the Western Mediterranean Region. The second region is the *Central and Southern Anatolia Region*, covering Konya, Karaman, Aksaray, Nigde, and Kayseri provinces and the Central and Eastern Mediterranean Regions. The third region corresponds to the

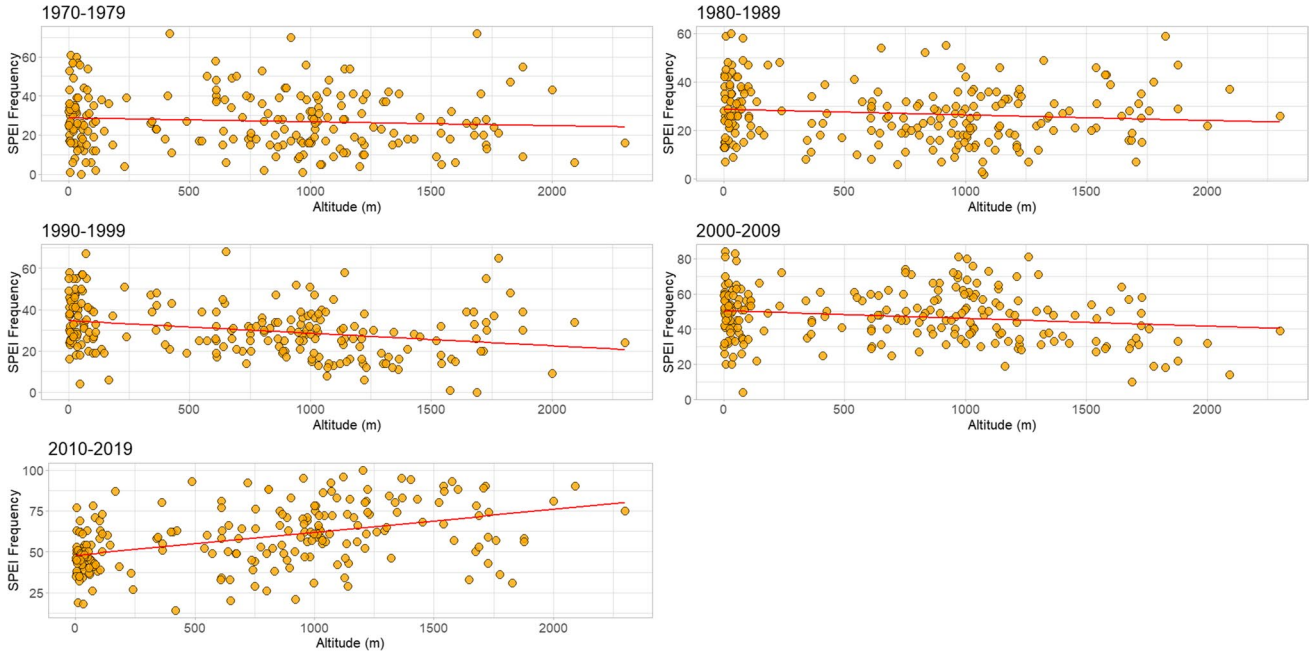


Fig. 7 Distribution of SPEI-12 values less than -0.5 by altitude through the period

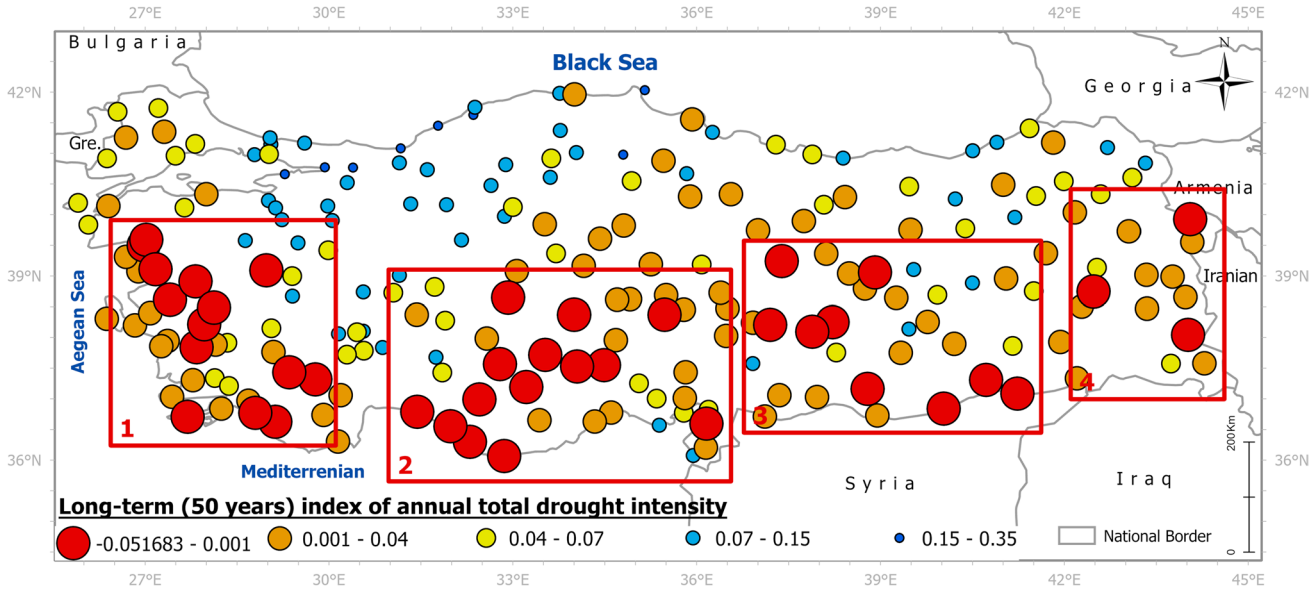


Fig. 8 Spatial distribution of drought intensity calculated by the SPEI-12 values using the run theory technique. The regions with red frames represent hotspots of drought intensity

Southeastern Anatolia Region. Finally, the fourth region encompasses the *Eastern Anatolia Region*, including the provinces of Igdir, Bitlis, and Van.

3.4 Drought trend's spatial pattern

The M–K trend test was utilized to determine the trends of SPEI values. The results of the M–K test indicate significant trends in 188 out of 222 stations. Among these stations, an increasing trend was observed in 13, while a decreasing trend was detected in 175 stations. No significant trend was found in the remaining 134 stations.

Figure 9 spatially presents the M–K trend test results and Sen's Slope coefficients at a 95% confidence level. The red triangle symbols in Fig. 9 represent stations where the M–K trend test results are significant, and Sen's Slope coefficients

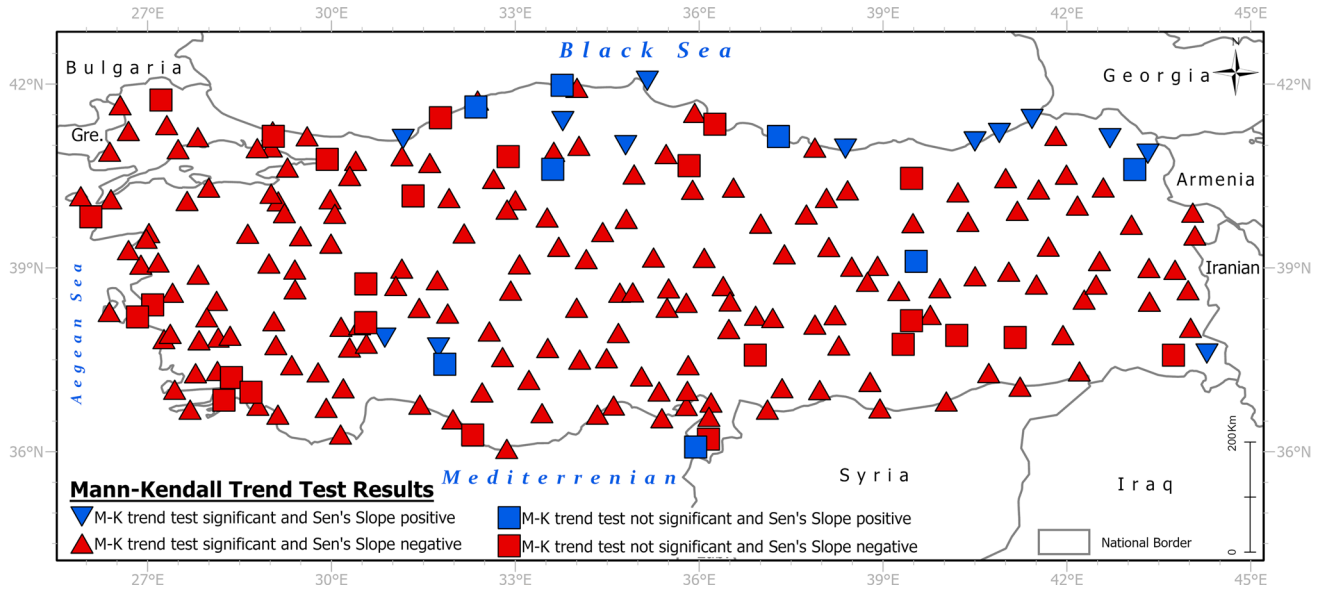


Fig. 9 Spatial distribution of the results of the Mann–Kendall trend test and Sen's Slope coefficients. Significant trends are represented by triangles, whereas non-significant trends are represented by squares. The blue hue indicates that Sen's Slope coefficients are positive, while the red color indicates that they are negative

are negative, indicating an increasing trend in drought, implying a worsening of drought conditions. Conversely, the blue triangle symbols indicate stations where the M–K trend test results are significant, and Sen's Slope coefficients are positive, signifying a decreasing trend in drought intensity. Moreover, stations indicated by square symbols did not exhibit a significant trend. However, even though the increase in drought is statistically significant (p-value less than 0.05) at the stations with blue triangle symbols, there is no deepening of the drought (Sen's Slope is positive). At the stations with square symbols, there is no discernible drought trend. Droughts are growing more severe because of this across much of Turkey. In other words, the drought is worsening across Turkey, except for the Black Sea Region, the Lakes Region, and the Ardahan-Kars Plateau, which is in northeastern Turkey.

4 Discussion

In this study, the spatial patterns of the years 1973, 1989, 1993, 1994, 2001, and 2008 were analyzed to examine the spatial characteristics of historically significant drought years in Turkey, as outlined in the literature. February was chosen to represent the winter period, and July was chosen to represent the summer period, focusing on drought conditions. The findings indicate that the spatial distribution of drought conditions in July is broader compared to February. Furthermore, an increase in the spatial extent of droughts over time was identified. Among the studied years, it was determined that 2001 and 2008 had relatively extensive drought coverage. During these periods, "moderately dry," "very dry," and "extremely dry" drought categories were observed to be predominant over a significant portion of the country. These findings partially parallel the results obtained by Akbaş (2014). Researchers examining specific drought years in Turkey using the PDSI method have defined the year 2008 as one of the years with the widest spatial coverage. Similarly, our findings exhibit a nearly consistent alignment with the results obtained by Dabanlı et al. (2017), who conducted drought analysis in Turkey using the SPI approach.

Throughout the examined time series, the highest drought frequency was observed at the Bozcaada station, while the lowest frequency was recorded at the Ispir station. These results demonstrate internal consistency considering the physical geography characteristics of both stations. Bozcaada is located in the western part of the country, along the coast, characterized by a Mediterranean climate associated with low rainfall and high temperatures. In contrast, Ispir, with an elevation exceeding 2000 m, exhibits characteristics of a semi-humid climate.

The spatial distribution pattern of drought frequencies analyzed in ten-year periods over time generally exhibits variation in each period. However, according to the results, it was determined that during the three-decade period between 1980 and 2009, the western, southern, and central regions of the country experienced higher drought frequencies. Moreover, it is noteworthy that from 2010 to 2019, the highest drought frequencies were predominantly observed in the high plateau areas of Anatolia. Overall, due to the

semi-arid and semi-humid climate characteristics of this extensive geography, further studies are needed to examine the increasing drought features in more detail in recent years.

To examine the relationship between drought and elevation, the distribution of drought concerning elevation was analyzed in ten-year periods. The results obtained indicate that there is no direct relationship between drought and elevation in Turkey. However, it was observed that from 2010 to 2019, a gradually increasing trend in drought occurs with elevation. The primary reason for this phenomenon is the low orographic precipitation rate in Turkey. As is generally known, at higher altitudes, temperatures decrease, increasing the probability of condensation. In this context, it would be a logical assumption that there is a positive relationship between elevation and precipitation. However, it's important to remember that the increase in precipitation with elevation may be limited to a certain height. This limitation is due to the decrease in water vapor in the air parcel, which is the fundamental reason behind this scenario. As a result, it could be a natural conclusion to predict that there is no significant relationship between elevation and drought. If the only factor influencing precipitation in this study was elevation, a correlation would be expected between elevation and drought. However, this study examines all precipitation factors. Furthermore, it can also be suggested that these findings might be related to global climate change. For instance, a study by Sen et al. (2012) that examines drought patterns in Turkey using projection data raises doubts about the existence of such a relationship. Therefore, in-depth investigations into drought characteristics in this field should be considered an important research topic in future studies.

The findings of drought intensity suggest that drought in Turkey exhibits a roughly increasing gradient from north to south. Similar patterns are observed in the M–K trend analyses. These test results indicate the deepening and intensification of drought in a significant part of Turkey. In this context, the Western, Central, and Southern Anatolian regions encompass the areas where high drought intensity is observed. These findings are in complete harmony with the results of Tatli and Türkeş (2011); Tatli (2015a, 2021); Serkendiz and Tatli (2023); and Serkendiz et al. (2023).

Turkey's vast geography hosts diverse climate conditions. Among these, the predominant climate type is the Mediterranean climate, characterized by dry and hot summers and mild and humid winters. The analyses conducted show that drought intensities in Turkey have increased, especially in regions influenced by the Mediterranean climate. A variety of climatic and geographical factors underlie the occurrence of severe drought events in these areas.

Turkey's climate is generally shaped by two main macro factors. The first involves air masses that are effective at different times of the year and is related to the general atmospheric circulation. The second factor concerns Turkey's physical geographical features, including physiographic characteristics, its continental position, vegetation cover, and density. During the summer months in Turkey, tropical-origin hot and dry air masses prevail, while in winter, cold and humid polar air masses dominate. The majority of Turkey's rainfall results from frontal precipitation caused by the convergence of these two different air masses. Additionally, midlatitude cyclones occurring in winter and early spring serve as significant sources of precipitation, particularly for the Aegean and Mediterranean regions (Almazroui et al. 2015). Turkey's physiographic features have a pronounced impact on rainfall formation and distribution. Particularly, mountain ranges running parallel to the northern and southern coasts, such as the North Anatolian Mountains and the Taurus Mountains, significantly influence rainfall distribution by obstructing the inland progression of humid air masses. Consequently, the inland regions surrounded by high mountain masses in the northern and southern directions receive insufficient rainfall. Similarly, the Southeastern Anatolia Region is located in a region far from the sea's influence and is particularly affected by extremely hot and dry air from the south, especially during the summer months. Therefore, the fundamental reason for these regions being significantly exposed to drought lies in their climatic and physiographical characteristics.

However, factors such as large-scale climate patterns such as the North Atlantic Oscillation (NAO) and El Niño can also affect drought in Turkey. For instance, studies conducted by Türkeş and Erlat (2003) and Tatli and Menteş (2019) demonstrate that especially the negative phase of NAO is a significant factor affecting the precipitation conditions of the Mediterranean basin, which includes Turkey. Furthermore, analyses conducted by Karabörk and Kahya (2003) show that Turkey's rainfall responds to El Niño and La Niña events occurring in the South Pacific Ocean, leading to detected variations in precipitation amounts. These situations can be related to understanding the drought trends in Turkey in the context of global climate change.

5 Conclusions

The comprehensive analysis of drought patterns in Turkey based on long-term meteorological data provides valuable insights into the country's climate dynamics. The results of this study reveal significant spatial and temporal variations in rainfall distribution, drought frequency, intensity, and trends across various regions of Turkey. The findings can be summarized as follows:

It was observed that the driest ten years in the selected stations occurred almost between 2000 and 2010 during the 1970–2019 period. Our findings indicate that each station experienced severe drought conditions for an average of

11 years during the analyzed 50-year period. Moreover, our results show that the durations of drought periods have increased over time. Specifically, the first period lasted for five years (1970–1975), the second period for ten years (1985–1995), and the third period for twenty years (2000–2019). The increasing duration of these drought periods can be explained by rising evapotranspiration rates associated with the increase in global temperatures.

Additionally, the seasonal distribution patterns of drought were represented by the selected six drought years (1973, 1989, 1993, 1994, 2001, and 2008) to capture the seasonal context of drought patterns in the time series. These analyses revealed how drought conditions changed over time in various regions of Turkey and which regions were more affected. Particularly, in 2001, severe drought conditions were observed with the broadest spatial extent across Turkey. These results provide crucial information for drought resilience strategies and water resource management in Turkey.

Bozcaada was identified as the station with the highest (223) drought frequency in northwestern Turkey, while Ispir in Erzurum province had the lowest (151) drought frequency. The findings illustrate spatial frequency patterns that varied over periods. For instance, in the 1970–1979 period, the Black Sea and Eastern Black Sea regions showed high frequencies, while the northwestern Anatolia region experienced a significant increase in the 1980–1989 period. In the 1990–2000 period, southwestern and western Turkey had high frequencies, whereas in the 2000–2009 period, the Central Anatolia and Eastern Mediterranean regions were affected.

The relationship between elevation and drought, while not significant in the 1970–2009 periods, indicates an increasing trend in drought as elevation rises in the 2010–2019 period.

The results indicated a gradual increase in drought intensity from north to south across Turkey. In this context, western, central, southern, and eastern regions of the country generally exhibited high drought intensities. The research results have identified four hotspots of drought regions in Turkey: (1) *Western Anatolia Region*, (2) *Central and Southern Anatolia Region*, (3) *Southeastern Anatolia Region*, and (4) *Eastern Anatolia Region.* On the other hand, the Black Sea region, Marmara region, and northwestern part of Central Anatolia exhibited low drought intensity. These results contribute significantly to understanding the drought patterns and affected regions in Turkey.

According to the results of the M–K trend analysis, significant trends were observed in 188 out of 222 stations. Among these stations, 13 exhibited an increasing trend, while a decreasing trend was detected in 175 stations. No significant trend was observed in the remaining 134 stations. These results indicate an overall increase in drought across much of Turkey.

These findings have critical implications for water resource management, agriculture, and ecosystem sustainability in Turkey. As drought events become more frequent and severe, adaptable measures and sustainable water management strategies are necessary to mitigate the socio-economic and environmental impacts of prolonged water scarcity. Moreover, comprehensive research and monitoring efforts are required to fully understand the complex interactions between climate change, rainfall patterns, and drought events for informed decision-making and flexible future planning.

Abbreviations *CRED*: Center for Research on the Epidemiology of Disasters; *EM-DAT*: Emergency Events Database; *IDW*: Inverse Distance Weighted; *IPCC*: Intergovernmental Panel on Climate Change; *M–K*: Mann–Kendall; *NAO*: North Atlantic Oscillation; *PDSI*: Palmer Drought Severity Index; *PET*: Potential Evapotranspiration; *SPEI*: Standardized Precipitation Evapotranspiration Index; *SPI*: Standardized Precipitation Index

Author contribution The study's design and development were aided by all the authors. Data collection, analysis, and figure creation and interpretation were handled by Hıdır Serkendiz, Hasan Tatli, and Ayşegül Kılıç. Hıdır Serkendiz wrote the initial manuscript at first, and Hasan Tatli corrected and commented on it later. Following that, all authors read the article and made the necessary changes and additions to ensure its approval.

Funding This work was supported by TUBITAK (The Scientific and Technical Research Council of Turkey-Project) within the scope of 1001—Scientific and Technological Research Projects Support Programme (No: 121O384).

Data availability On reasonable request, data supporting the findings of this study can be obtained from the Turkish State Meteorological Service (https://www.mgm.gov.tr/eng/forecast-cities.aspx).

Code availability The SPEI package's source code written in R was used for SPEI calculation. The graphics source codes in R language can be shared upon request.

Declarations

Competing interests The authors declare no competing interests.

Ethics approval Not applicable.

Consent to participate Not applicable.

Consent to publication Not applicable.

References

Akbaş A (2014) Important drought years over Turkey. Turkish J Geogr Sci 12:101–118. https://doi.org/10.1501/Cogbil_0000000155

Almazroui M, Awad AM, Islam MN, Al-Khalaf AK (2015) A climatological study: wet season cyclone tracks in the East Mediterranean region. Theor Appl Climatol 120:351–365. https://doi.org/10.1007/s00704-014-1178-z

Baydaroğlu Yeşilköy O, Koçak K, Şaylan L (2021) Prediction of commonly used drought indices using support vector regression powered by chaotic approach. Italian J Agrometeorology 2:65–76. https://doi.org/10.13128/ijam-970

CRED (2020) Human cost of disasters: An overview of the last 20 years. Centre for Research on the Epidemiology of Disasters, Brussels

Cressie N (1990) The Origins of Kriging. Math Geol 22:239–252. https://doi.org/10.1007/BF00889887

Dabanlı İ, Mishra AK, Şen Z (2017) Long-term spatio-temporal drought variability in Turkey. J Hydrol 552:779–792. https://doi.org/10.1016/j.jhydrol.2017.07.038

Erinç S (1993) Outlines of Turkey's Physical Geography. Istanbul Univ Inst Marine Sci Geography Bullet 10:1–10 (in Turkish)

Hamzah FB, Hamzah FM, Razali SM, Samad H (2021) A comparison of multiple imputation methods for recovering missing data in hydrological studies. Civil Eng J 7(9):1608–1619. https://doi.org/10.28991/cej-2021-03091747

Hirsch RM, Alexander RB, Smith RA (1991) Selection of methods for the detection and estimation of trends in water quality. Water Resour Res 27:803–813. https://doi.org/10.1029/91WR00259

IPCC (2021) Summary for Policymakers. In: Masson-Delmotte V, Zhai P, Pirani A, Connors SL, Péan C, Berger S, Caud N, Chen Y, Goldfarb L, Gomis MI, Huang M, Leitzell K, Lonnoy E, Matthews JBR, Maycock TK, Waterfield T, Yelekçi O, Yu R, Zhou B (eds) Climate Change 2021: The Physical Science Basis. Contribution of Working Group I to the Sixth Assessment Report of the Intergovernmental Panel on Climate Change. in press

Junninen H, Niska H, Tuppurainen K, Ruuskanen J, Kolehmainen M (2004) Methods for imputation of missing values in air quality data sets. Atmos Environ 38(18):2895–2907. https://doi.org/10.1016/j.atmosenv.2004.02.026

Karabörk MÇ, Kahya E (2003) The teleconnections between the extreme phases of the southern oscillation and precipitation patterns over Turkey. Int J Climatol 23:1607–1625. https://doi.org/10.1002/joc.958

Kendall MG (1975) Rank Correlation Methods, 4th edn. London, Charles Griffin

Koç T (2013) Morphometric Characteristics of Turkey. In: Öner E (ed) Gift to Professor İlhan Kayan. Aegean University Publications, Izmir, pp 435–470 (in Turkish)

Liu C, Yang C, Yang Q, Wang J (2021) Spatiotemporal drought analysis by the standardized precipitation index (SPI) and standardized precipitation evapotranspiration index (SPEI) in Sichuan Province, China. Sci Rep 11:1–24. https://doi.org/10.1038/s41598-020-80527-3

Mann HB (1945) Non-parametric test against trend. Econometrica 13:245–259

Matheron G (1963) Principles of geostatistics. Econ Geol 58(8):1246–1266. https://doi.org/10.2113/gsecongeo.58.8.1246

McKee TB, Doesken NJ, Kleist J (1993) The relationship of drought frequency and duration to time scales. In: Proceedings of the Eighth Conference on Applied Climatology (vol 17, no. 22). Anaheim, California

Mishra AK, Singh VP (2010) A review of drought concepts. J Hydrol 391:202–216. https://doi.org/10.1016/j.jhydrol.2010.07.012

Moral FJ (2010) Comparison of different geostatistical approaches to map climate variables: application to precipitation. Int] J Climatol: J Royal Meteol Soc 30(4):620–631. https://doi.org/10.2307/1907187

Palmer WC (1965) Meteorological Drought. Research Paper, Washington, D.C.

Peel MC, Finlayson BL, McMahon TA (2007) Updated world map of the Köppen-Geiger climate classification. Hydrol Earth Syst Sci 11:1633–1644. https://doi.org/10.5194/hess-11-1633-2007

Schneider T (2001) Analysis of incomplete climate data: Estimation of mean values and covariance matrices and imputation of missing values. J Clim 14(5):853–871

Sen B, Topcu S, Türkeş M, Warner JF (2012) Projecting climate change, drought conditions and crop productivity in Turkey. Climate Res 52:175–191. https://doi.org/10.3354/cr01074

Serkendiz H, Tatli H (2023) Assessment of multidimensional drought vulnerability using exposure, sensitivity, and adaptive capacity components. Environ Monit Assess 195:1154. https://doi.org/10.1007/s10661-023-11711-x

Serkendiz H, Tatli H, Özcan H, Çetin M, Sungur A (2023) Multidimensional assessment of agricultural drought vulnerability based on socioeconomic and biophysical indicators. Int Journal of Disaster Risk Reduction 98:104121. https://doi.org/10.1016/j.ijdrr.2023.104121

Tatli H (2015a) Downscaling standardized precipitation index via model output statistics. Atmósfera 28:83–98. https://doi.org/10.1016/S0187-6236(15)30002-3

Tatli H (2015b) Detecting persistence of meteorological drought via the Hurst exponent. Meteorol Appl 22(4):763–769

Tatli H (2021) Multivariate-drought indices—case studies with observations and outputs of NCAR CCSM-4 ensemble models. Theoret Appl Climatol. https://doi.org/10.1007/s00704-021-03736-4

Tatli H, Dalfes HN (2020) Long-Time Memory in Drought via Detrended Fluctuation Analysis. Water Resour Manage 34:1199–1212. https://doi.org/10.1007/s11269-020-02493-9

Tatli H, Menteş ŞS (2019) Detrended cross-correlation patterns between North Atlantic oscillation and precipitation. Theor Appl Climatol 138:387–397. https://doi.org/10.1007/s00704-019-02827-7

Tatli H, Türkeş M (2011) Empirical Orthogonal Function analysis of the palmer drought indices. Agric for Meteorol 151:981–991. https://doi.org/10.1016/j.agrformet.2011.03.004

Tekin MK, Tatli H, Koç T (2021) Climate classification in Turkey: a case study evaluating Holdridge life zones. Theor Appl Climatol 144:661–674. https://doi.org/10.1007/s00704-021-03565-5

Thornthwaite CW (1948) An Approach toward a Rational Classification of Climate. Geogr Rev 38:55–94

Türkeş M (1990) Drought Regions and Important Drought Years in Turkey. PhD Thesis, Institute of Marine Sciences and Geography in Istanbul University, Advisor: Prof. Dr. Korkut Ata SUNGUR (in Turkish)

Türkeş M, Erlat E (2003) Precipitation changes and variability in Turkey linked to the North Atlantic oscillation during the period 1930–2000. Int J Climatol 23:1771–1796. https://doi.org/10.1002/joc.962

Türkeş M, Tatli H (2009) Use of the standardized precipitation index (SPI) and a modified SPI for shaping the drought probabilities over Turkey. Int J Climatol 29:2270–2282. https://doi.org/10.1002/joc.1862

Türkeş M, Akgündüz AS, Demirörs Z (2009) Drought periods and severity over the Konya Sub-region of the Central Anatolia Region according to the Palmer Drought Index. J Geogr Sci 7:129–144. https://doi.org/10.1501/Cogbil_0000000102. (in Turkish)

Turp MT, Öztürk T, Türkeş M, Kurnaz ML (2014) Regcm4.3.5 Investigation of Projected Changes for Near Future Air Temperature and Precipitation Climatology of Turkey and Surrounding Regions by Using the Regional Climate Model. Aegean Geogr J 23:1–24 (in Turkish)

UNDRR (2022) Global Assessment Report on Disaster Risk Reduction 2022: Our World at Risk: Transforming Governance for a Resilient Future. United Nations Office for Disaster Risk Reduction, Geneva

Vicente-Serrano SM, Beguería S, López-Moreno JI (2010) A Multiscalar Drought Index Sensitive to Global Warming: The Standardized Precipitation Evapotranspiration Index. J Clim 23:1696–1718. https://doi.org/10.1175/2009JCLI2909.1

Wilhelmi OV, Wilhite DA (2002) Assessing Vulnerability to Agricultural Drought: A Nebraska Case Study. Nat Hazards 25:37–58

Wilhite DA (1993) Chapter 1 The Enigma of Drought. In: Wilhite DA (ed) Drought assessment, management, and planning: Theory and case studies. Kluwer Academic Publishers, Boston, London, pp 3–16

Wilhite DA (2000) Chapter 1 Drought as a Natural Hazard: Concepts and Definitions. In: Wilhite DA (ed) Drought: A global assessment. Routledge, London, pp 1–21

Yevjevich V (1967) An objective approach to definitions and investigations of continental hydrologic droughts. Hydrology Papers August No. 23, Colorada State University, Fort Collins, Colorado

Zarei AR, Mahmoudi MR (2021) Influence of human activities on meteorological drought and its trends in Iran. Arab J Geosci 14. https://doi.org/10.1007/s12517-021-07287-w

Zarei AR, Mokarram M, Mahmoudi MR (2023a) Comparison of the capability of the Meteorological and Remote Sensing Drought Indices. Water Resour Manage 37:769–796. https://doi.org/10.1007/s11269-022-03403-x

Zarei AR, Mahmoudi MR, Moghimi MM (2023b) Determining the most appropriate drought index using the random forest algorithm with an emphasis on agricultural drought. Nat Hazards 115:923–946. https://doi.org/10.1007/s11069-022-05579-2

Publisher's Note Springer Nature remains neutral with regard to jurisdictional claims in published maps and institutional affiliations.

Springer Nature or its licensor (e.g. a society or other partner) holds exclusive rights to this article under a publishing agreement with the author(s) or other rightsholder(s); author self-archiving of the accepted manuscript version of this article is solely governed by the terms of such publishing agreement and applicable law.